Symmetry of Valence States of Heusler Compounds Explored by Linear Dichroism in Hard-X-Ray Photoelectron Spectroscopy

Siham Ouardi, Gerhard H. Fecher,* Xeniya Kozina, Gregory Stryganyuk, Benjamin Balke, and Claudia Felser
Institut für Anorganische und Analytische Chemie, Johannes Gutenberg–Universität, 55099 Mainz, Germany

Eiji Ikenaga, Takeharu Sugiyama, Naomi Kawamura, and Motohiro Suzuki
Japan Synchrotron Radiation Research Institute, SPring-8, Hyogo 679-5198, Japan

Keisuke Kobayashi
National Institute for Materials Science, SPring-8, Hyogo 679-5148, Japan
(Received 13 August 2010; published 12 July 2011)

This study reports on the linear dichroism in angular-resolved photoemission from the valence band of the Heusler compounds $NiTi_{0.9}Sc_{0.1}Sn$ and NiMnSb. High-resolution photoelectron spectroscopy was performed with an excitation energy of $h\nu = 7.938$ keV. The linear polarization of the photons was changed using an in-vacuum diamond phase retarder. The valence band spectra exhibit the typical structure expected from first-principles calculations of the electronic structure of these compounds. Noticeable linear dichroism is found in the valence band of both materials, and this allows for a symmetry analysis of the contributing states. The differences in the spectra are found to be caused by symmetry-dependent angular asymmetry parameters, and these occur even in polycrystalline samples without preferential crystallographic orientation.

DOI: 10.1103/PhysRevLett.107.036402 PACS numbers: 71.20.Lp, 79.60.−i

Photoelectron spectroscopy is of great importance in many fields of research because of its numerous advantageous properties [1–3]. Among its various applications, in particular, it is used to investigate the symmetries of the electronic structure of various materials. However, thus far, such studies have been restricted to atoms, molecules, adsorbates, and surfaces because low-energy (<1 keV) electrons have limited probing depths. This is disadvantageous in that three-dimensional (3D) bulk states cannot be studied. We demonstrate that this drawback can be eliminated by using hard x rays with variable polarization for excitation. In this study, we investigate this issue using Heusler compounds, which have attracted considerable interest in the fields of theory, thermoelectrics, and spintronics.

The linear dichroism in the angular distribution (LDAD) of photoelectrons has attracted considerable interest as a powerful probe to study the symmetry, orientation, and alignment phenomena in photoionization [4–6]. The prerequisites for this effect are the orientation of the photons and the alignment of the electronic states [7]. The first is realized by the linear polarization of the photons whereas the second might be produced by the alignment of the molecular axes or by the symmetry of the bands in a solid. The main difference between linear and circular dichroism in the angular distribution is that the former does not require a chirality or magnetization of the investigated system because the electric field vector of linearly polarized photons is a real vector whereas the helicity of circularly polarized photons is a pseudovector [8].

Angle-resolved photoelectron spectra excited by linearly polarized photons indicated that the intensities of emissions from chemisorbed systems exhibited strong variations [9]. Later, a dichroism with linearly polarized light was predicted, where the electric field vector is aligned at $\pm 45°$ with respect to the plane of incidence [8]. Subsequently, many theoretical [10] and experimental studies of the LDAD have been carried out. The basic theory of LDAD was first developed for gas-phase molecules and molecules adsorbed on surfaces [11]. LDAD measurements have been actively used to study different adsorbates as well as surfaces [6,12]. High asymmetries were reported for the valence orbitals of CO/Pt(111) [13]. The nonmagnetic and nonchiral system 1T-TaS_2 is an example of LDAD from solids [5].

Thus far, most studies dealing with LDAD have been based on soft radiation in the range from the vacuum ultraviolet region (ultraviolet photoelectron spectroscopy) to the soft-x-ray region [x-ray photoelectron spectroscopy (XPS)], resulting in a very limited probing depth that is suitable only for the examination of surface effects. Therefore, LDAD from real 3D bulk states has not yet been observed. In contrast, the use of hard x rays for excitation results in the emission of electrons having high kinetic energies, in turn leading to a high probing depth because of the increased electron mean free path. Recently, hard-x-ray photoelectron spectroscopy (HAXPES) has emerged as a powerful tool to investigate the electronic structure of solids [14] as well as multilayer systems [15,16] and the valence band of buried thin films [17].

The valence transitions of several bulk systems were successfully investigated by means of HAXPES [12,18,19], and, very recently, the polarization dependence of the emission from Au and Ag samples was reported [20].

In the present work, a combination of the LDAD with the bulk-sensitive HAXPES technique was used to investigate the symmetry of the valence states of nonmagnetized, polycrystalline Heusler compounds. The valence electronic structure of the Heusler compounds is easily changed by varying the composition. The compounds $NiTi_{0.9}Sc_{0.1}Sn$ and NiMnSb were selected in this study. The comparison of those allows to follow the change of the d valence bands when Mn d^5 is replaced by Ti d^2 [in practice, $(Ti_{0.9}Sc_{0.1})$-$d^{1.9}$]. NiMnSb was suggested to be a half-metallic ferromagnet [21]. The samples used for the HAXPES measurements were in the virgin state. NiTiSn is supposed to be a semiconductor [22]; therefore, this sample was heavily hole doped by Ti $\leftrightarrow$ Sc substitution with a composition of $NiTi_{0.9}Sc_{0.1}Sn$. This ensures that the Fermi energy clearly lies in the valence band and it suppresses unwanted *in-gap* states that were reported previously [23]. The details of the sample production and characterization are reported in Ref. [24]. Polycrystalline samples were cut to disks and the surface was polished. The sample surfaces were prepared by Ar^+ bombardment to remove traces of oxidation. Their cleanness was checked by regular low-energy XPS (Al $K\alpha$).

Hard-x-ray photoelectron spectroscopy was used as a bulk-sensitive probe [17] to study the valence band of the samples. The HAXPES experiment was performed using the beam line BL47XU at SPring-8 (Japan) [15]. Photons having an energy of 7.938 keV that were linearly polarized in the horizontal (p) and vertical (s) directions were used for selective excitation. The p polarized light was obtained from an undulator source without the use of any polarization optics. An in-vacuum phase retarder based on a 200 μm thick diamond crystal was used to rotate the linear polarization into the vertical plane. The degrees of polarization were $P_L = (I_h - I_v)/(I_h + I_v) = 0.99$ for p polarization and -0.7 to -0.9 for s polarization, where I_h and I_v denote the x-ray intensities of the horizontal and vertical polarization components, respectively. The kinetic energy of the photoemitted electrons was analyzed using a hemispherical analyzer (VG-Scienta R4000-12 kV). The overall energy resolution was set to 150 or 250 meV, as verified by the spectra obtained at the Fermi edge of a Au sample. The angular resolution was set to 2°. The angle between the electron spectrometer and photon propagation was fixed at 90°. The detection angle was set to $\theta = 2°$ in order to reach a near-normal emission mode. The angle of incidence of $\alpha = 88°$ ensures that the polarization vector of the linearly polarized photons is either nearly parallel (p) or perpendicular (s) to the surface normal. The use of the phase retarder for s polarized light considerably decreases the overall intensity because of the absorptivity of the diamond crystal. The integration of the count rate over the valence band of $NiTi_{0.9}Sc_{0.1}Sn$ results in a ratio of $I^p/I^s \approx 20$ when p polarization without the phase retarder is compared with s polarization with the retarder. Therefore, the spectra were normalized to the secondary background at energies below the valence band [25].

Figure 1 compares the valence band spectra and calculated electronic structure of $NiTi_{0.9}Sc_{0.1}Sn$ [25]. The density of states (DOS) exhibits a typical 4-peak structure in the energy range of the d states as well as the split-off s band with a_1 symmetry. These structures can be clearly observed in the photoelectron spectra. The sum of the polarization-resolved spectra corresponds to a spectrum with unpolarized photons. The width of the d part of the density of states (0 to -5 eV) corresponds to the width of the measured spectra. The spectrum exhibits a rather high intensity in the s part below (-7 eV) that is caused by the higher cross section for s states as compared to that for d states at a high excitation energy. The intensity of the d states is governed by the states localized at the Ni atoms. Dirac-Fock calculations for the photoexcitation of Ni, Ti, and Sc valence electrons indicate that at $h\nu = 8$ keV, the cross section for Ni 3d states is 20 times higher than that for light 3d transition metals.

It is evident that striking differences appear in the spectra if the polarization is changed from p to s. The spectra shown in Fig. 1 indicate that the s states have a higher intensity for p polarization and the s polarization result in a

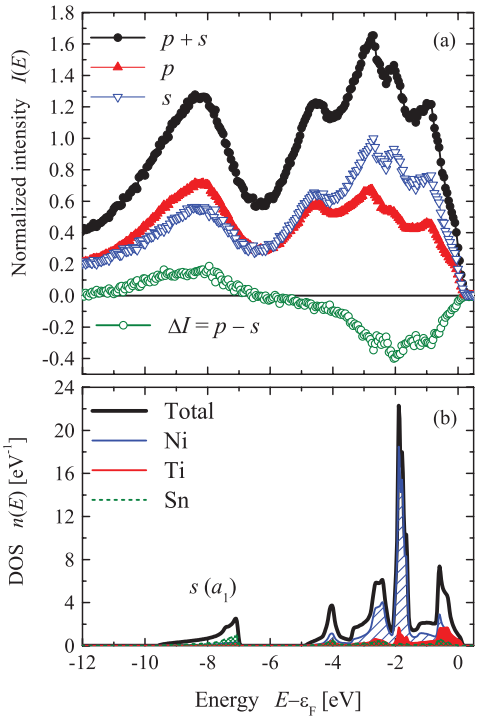

FIG. 1 (color). Electronic structure and polarization-dependent photoelectron spectra of $NiTi_{0.9}Sc_{0.1}Sn$. (a) Spectra obtained with s and p polarized light together with the sum and difference and (b) total and partial density of states (DOS). Note that the Sc substitution creates holes, its d states appear in the unoccupied part above the band gap.

higher intensity in the energy range of the d states. In particular, the intensity of the Ni $3d$ states at -2 eV is enhanced and the structure of the d states becomes better resolved under illumination with s polarized photons.

With a change from $NiTi_{0.9}Sc_{0.1}Sn$ to NiMnSb, and thus, from Ti $3d^2$ to Mn $3d^5$, one expects a change in the spectra in the energy range of the d states. Figure 2 shows a comparison of the valence band spectra and the electronic structure of NiMnSb [25]. The DOS exhibits a 5-peak structure in the range of the d states that is not completely resolved in the spectra. A pronounced maximum appears at approximately -3 eV in the DOS and spectra. It emerges from the Mn t_2 states that are responsible for the localized magnetic moment in NiMnSb. The changes in the spectra while changing the polarization are the same as those observed for $NiTi_{0.9}Sc_{0.1}Sn$. Again, the intensity of the Ni $3d$ states at -2 eV is noticeably enhanced for s polarized photons. The intensity of the Mn $3d$ states is enhanced in a similar manner.

The polarization-dependent spectra can be most easily analyzed for direct emission by neglecting all final state effects in the first step (for example, electron diffraction [3]). In the dipole approximation, the observed intensity ($I \propto \frac{d\sigma}{d\Omega}$) depends on the partial cross section (σ_κ) and the angular asymmetry parameter (β_κ) of the photoexcited states. κ assigns a complete set of quantum numbers describing the initial state. For atomiclike states in a single electron description, these are $\kappa = n, l$ with main quantum number n and orbital angular momentum l. In the case of linearly polarized photons, the angular dependence of the intensity in the dipole approximation is given as follows [26]: $I_\kappa^{E_1}(\theta) = \sigma_\kappa[1 + \beta_\kappa P_2(\theta)]$, where $P_2(\theta) = (3\cos^2\theta - 1)/2$ is the second Legendre polynomial and θ is measured with respect to the electric field vector. The angular parameter is limited to the range $-1 \le \beta \le 2$. Both parameters, σ_κ and β_κ, depend on the kinetic energy of the emitted electrons. In addition, higher-order nondipole terms may appear (M_1 and E_2 transitions) in addition to the E_1 transitions. The first-order nondipole approximation results in an additional term $I_\kappa^{M_1,E_2} \propto \sigma_\kappa[(\delta_\kappa + \gamma_\kappa\cos^2\theta)\sin\theta\cos\phi]$ in the angular distribution [27], with the angular parameters γ_κ and δ_κ that depend on the magnetic dipole and electric quadrupole matrix elements. Note that δ has to vanish if $\beta = 2$ or -1.

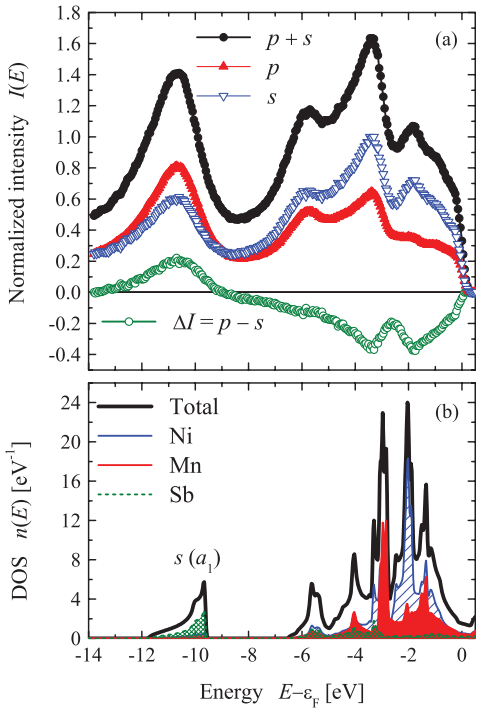

FIG. 2 (color). Electronic structure and polarization-dependent photoelectron spectra of NiMnSb. (a) and (b) as in Fig. 1.

In the present case, where the emitted electrons are either parallel (p) or perpendicular (s) to the electric field vector, the intensities are given by

$$I_\kappa^p \propto \sigma_\kappa(1 + \beta_\kappa), \qquad I_\kappa^s \propto \sigma_\kappa\left(1 + \delta_\kappa - \frac{\beta_\kappa}{2}\right). \tag{1}$$

For s polarization, positive values of δ enhance and negative values attenuate the intensity. For atoms or linear molecules, the dipole asymmetry parameter for s electrons is $\beta_{n0} = 2$ in the nonrelativistic approximation, implying $\delta_{n0} = 0$.

Neglecting an incomplete polarization, in the geometry used, $\beta_0 = 2$ should lead to a vanishing intensity for excitation of the s states by s polarized photons; however, this is clearly not the case. In the solid with T_d symmetry, however, the photoexcitation of the s band is better described by a $a_1 \rightarrow t_2$ transition as compared to an atom in which one simply has transitions into final p states [28,29]. Restricting the partial waves of the initial a_1 state to $l = 0$ will allow already direct transitions into partial waves with $l' = 1, 2$ of the final t_2 state, and the β parameter becomes [30]

$$\beta_{a_1,l=0} = \frac{2D^2_{t_2,l'=1} - 6/7D^2_{t_2,l'=2}}{D^2_{t_2,l'=1} + D^2_{t_2,l'=2}}, \tag{2}$$

where D are the radial matrix elements. The additional $D_{t_2,l'=2}$ term immediately allows for $\beta_{a_1,l=0} < 2$.

Generally, the angular dependence of the final state contains contributions from much higher l' values that are compatible with the irreducible representations of the T_d symmetry group. Indeed, because of polycrystalline samples without preferential crystallographic directions, a rather uniform contribution is expected. This affects not only the angular distribution of the emission from the initial a_1 states but also that of the e and t_2 states.

From the enhancement of the intensity from the d states with s polarized light, one would expect negative β_{3d} parameters because the restriction on the nondipole parameter to $\delta \le 1 - \beta/2$ (for $\beta > 0$) [31] does not allow for I_{3d}^s to become larger than I_{3d}^p, at least for direct emission. The calculated atomic-type β_{3d} parameters for Ni and Mn are in the range of 1.16 to 1.28, but they are

not negative [25]. Assuming more complete $e \rightarrow (t_1, t_2)$ and $t_2 \rightarrow (a_1, e, t_1, t_2)$ dipole transitions, the differences become obvious [25]. The equation for $\beta_{e,l=2}$ and $\beta_{t_2,l=2}$, however, cannot be given as easily as above for $\beta_{a_1,l=0}$ without accounting for the contributions of l other than the 2 that are present in the initial e and t_2 states. In NiMnSb, the Mn states at -3 eV have a nearly pure t_2 character, whereas the Ni d states of both compounds at -2 eV have t_2 as well as e characters. A detailed analysis reveals that the relative change in the intensity in NiMnSb is clearly higher at -2 eV ($\approx 30\%$) as compared to that at -3 eV ($\approx 20\%$), even without any background subtraction. Similarly, in $NiTi_{0.9}Sc_{0.1}Sn$, the relative change is slightly higher at approximately -1 eV. At -1 eV, most states have e character whereas at -3 eV the states mainly have t_2 character. The variation of the relative changes for both compounds with differences observed over the entire valence band clearly indicates a symmetry dependence of the angular asymmetry parameters.

In the present study, LDAD in hard-x-ray photoelectron spectroscopy was used to study the angular asymmetry in photoemission from the valence states of polycrystalline Heusler compounds. The polarization-dependent measurements reveal that even high energies and polycrystalline samples do not yield a one-to-one correspondence of photoemission spectra and density of states. This is mainly because there not only exist differences in the partial cross sections, but there also exists the symmetry dependence of the angular asymmetry parameters. It was shown that the change in the linear polarization allows for different states of the valence band of complex materials to be easily distinguished. The polarization-dependent HAXPES experiments can clearly be applied not only to valence states but also to core states. Overall, the high bulk sensitivity of HAXPES combined with linearly polarized photons will have a major impact on the study of the electronic structure of bulk materials, thin films, deeply buried materials, and interfaces.

The financial support by DfG (TP 1.3-A of Research Unit FOR 1464) and DfG-JST (FE633/6-1) is gratefully acknowledged. The synchrotron radiation measurements were performed at BL-47XU with the approval of the Japan Synchrotron Radiation Research Institute (JASRI) (Proposal No. 2009B0017).

*fecher@uni-mainz.de

[1] K. Kobayashi, Nucl. Instrum. Methods Phys. Res., Sect. A **547**, 98 (2005).
[2] K. Siegbahn, Nucl. Instrum. Methods Phys. Res., Sect. A **547**, 1 (2005).
[3] C. S. Fadley, Nucl. Instrum. Methods Phys. Res., Sect. A **547**, 24 (2005).
[4] A. Oelsner, G. H. Fecher, C. Ostertag, T. Jentzsch, and G. Schönhense, Surf. Sci. **331–333**, 349 (1995).
[5] T. Matsushita *et al.*, Phys. Rev. B **56**, 7687 (1997).
[6] G. H. Fecher *et al.*, J. Electron Spectrosc. Relat. Phenom. **88–91**, 185 (1998).
[7] A. Oelsner, G. H. Fecher, M. Schicketanz, and G. Schönhense, Surf. Sci. **433-435**, 53 (1999).
[8] N. A. Cherepkov and G. Schönhense, Europhys. Lett. **24**, 79 (1993).
[9] R. J. Smith, J. Anderson, and G. J. Lapeyre, Phys. Rev. Lett. **37**, 1081 (1976).
[10] N. M. Kabachnik, J. Electron Spectrosc. Relat. Phenom. **79**, 269 (1996).
[11] N. A. Cherepkov and G. Raseev, J. Chem. Phys. **103**, 8238 (1995).
[12] V. V. Kuznetsov, N. A. Cherepkov, G. H. Fecher, and G. Schönhense, J. Chem. Phys. **110**, 9997 (1999).
[13] C. Ostertag, J. Bansmann, C. Grünewald, T. Jentzsch, A. Oelsner, G. H. Fecher, and G. Schönhense, Surf. Sci. **331–333**, 1197 (1995).
[14] Detailed reviews of the method are found in *Proceedings of the Workshop on Hard X-Ray Photoelectron Spectroscopy*, edited by J. Zegenhagen and C. Kunz [Nucl. Instrum. Methods Phys. Res., Sect. A 547, No. 1 (2005)].
[15] K. Kobayashi, Nucl. Instrum. Methods Phys. Res., Sect. A **601**, 32 (2009).
[16] S. Ueda *et al.*, Phys. Rev. B **80**, 092402 (2009).
[17] G. H. Fecher *et al.*, Appl. Phys. Lett. **92**, 193513 (2008).
[18] H. Sato *et al.*, Physica (Amsterdam) **351B**, 298 (2004).
[19] G. Panaccione *et al.*, J. Phys. Condens. Matter **17**, 2671 (2005).
[20] A. Sekiyama *et al.*, New J. Phys. **12**, 043045 (2010).
[21] R. A. de Groot, F. M. Müller, P. G. van Engen, and K. H. J. Buschow, Phys. Rev. Lett. **50**, 2024 (1983).
[22] F. G. Aliev, Physica (Amsterdam) **171B**, 199 (1991).
[23] K. Miyamoto *et al.*, Appl. Phys. Express **1**, 081901 (2008).
[24] S. Ouardi *et al.*, Phys. Rev. B **82**, 085108 (2010).
[25] See Supplemental Material at http://link.aps.org/supplemental/10.1103/PhysRevLett.107.036402 for a description of normalization of spectra and details of calculations.
[26] J. Cooper and R. N. Zare, J. Chem. Phys. **48**, 942 (1968).
[27] J. W. Cooper, Phys. Rev. A **42**, 6942 (1990).
[28] V. V. Kuznetsov, N. A. Cherepkov, G. H. Fecher, and G. Schönhense, J. Chem. Phys. **117**, 7180 (2002).
[29] G. H. Fecher, V. V. Kuznetsov, N. A. Cherepkov, and G. Schönhense, J. Electron Spectrosc. Relat. Phenom. **122**, 157 (2002).
[30] N. Chandra, J. Phys. B **20**, 3417 (1987).
[31] O. Hemmers, R. Guillemin, and D. W. Lindle, Radiat. Phys. Chem. **70**, 123 (2004).